

Supporting Information

for

Multi-stimuli-responsive aggregation-induced emission of boryl substituted phenothiazine

*Guoqiang Li,^{‡a} Yan Wang,^{‡a} Yaohui Li,^a Zengheng Wen,^a Zhuang Luo,^a Weijun Song,^{*a}
and Weidong Zhang^{*a}*

^a School of Chemical Engineering, Qinghai University, Xining, 810016, China

E-mail: zhangwd@qhu.edu.cn; songweijun1980@163.com

Contents

| | |
|--|----|
| 1. The excitation and emission spectra | 3 |
| 2. The fluorescence lifetime decay spectra..... | 3 |
| 3. The Experimental and the Calculated UV-Vis spectra..... | 4 |
| 4. Aggregation-induced fluorescence properties | 15 |
| 5. Electrochemical properties | 19 |
| 6. Comparison of HOMO/LUMO plots..... | 20 |
| 7. Determination of the detection limit..... | 23 |
| 8. Reversibility of the MFC performance..... | 23 |
| 9. ¹ H NMR and ¹³ C NMR spectra..... | 24 |
| 10. HRMS spectra..... | 28 |
| 11. Reference | 30 |

1. The excitation and emission spectra

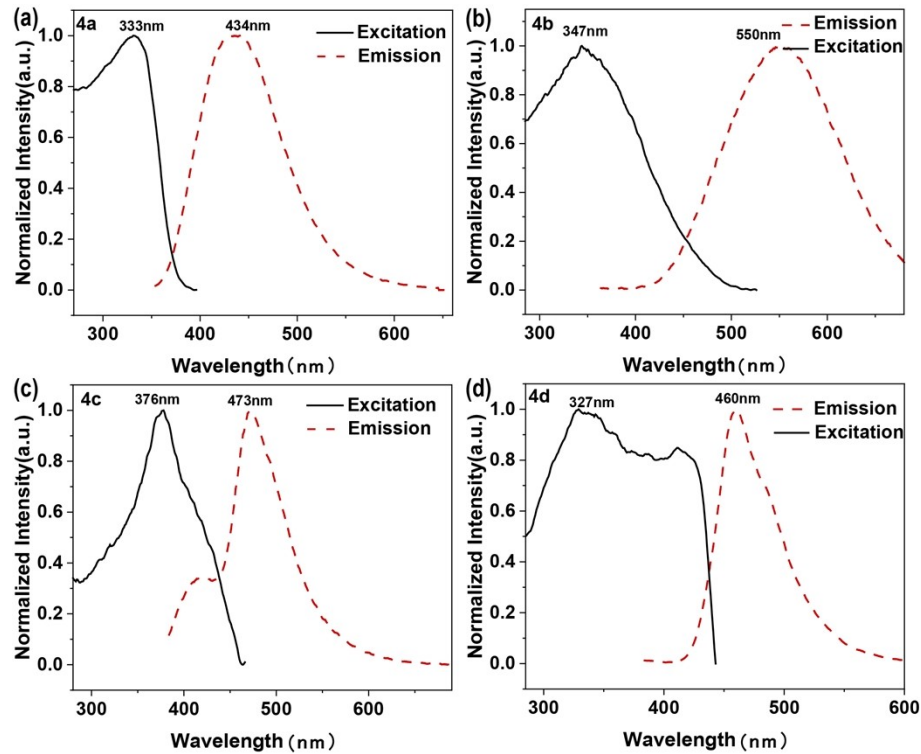


Figure S1. Fluorescence excitation (solid line) and emission spectra (dashed line).

2. The fluorescence lifetime decay spectra

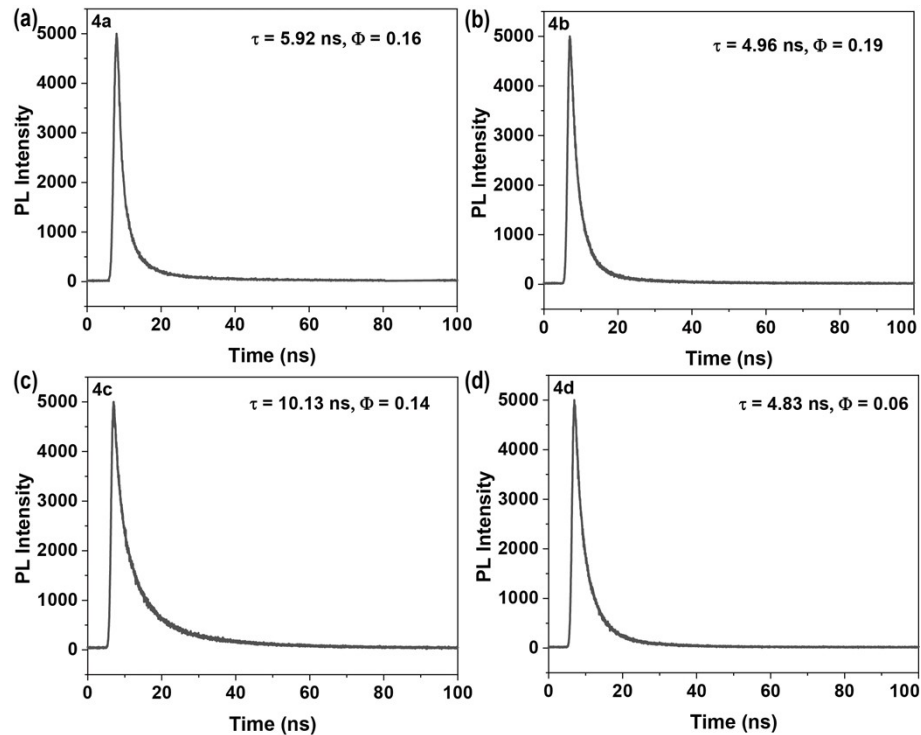


Figure S2. Fluorescence lifetime decay spectra of **4a-4d**.

3. The Experimental and the Calculated UV-Vis spectra

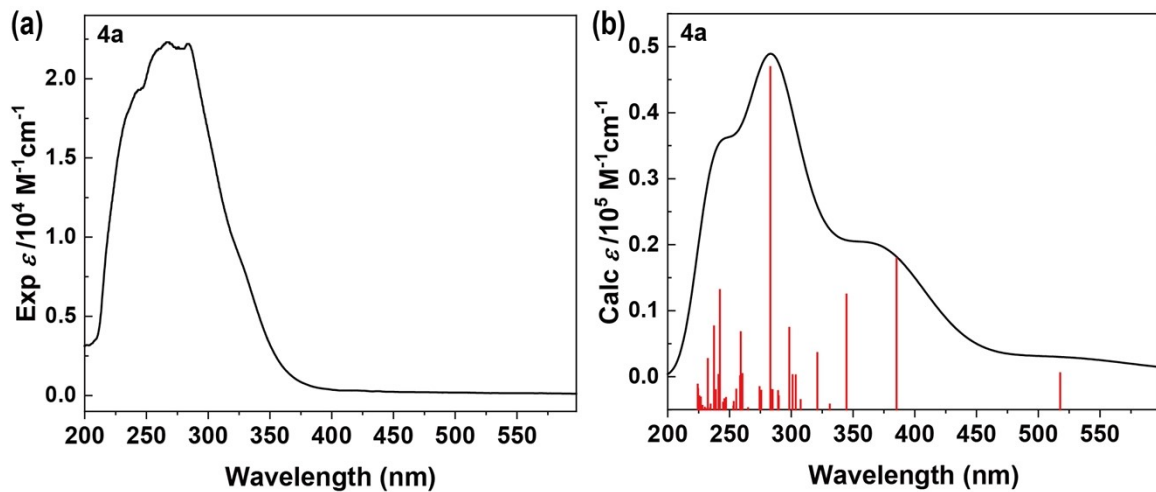


Figure S3. Computed, at the TD-DFT, B3LYP-D3/6-31g(d),¹⁻⁴ level of theory and experimental UV-vis spectra of **4a**.

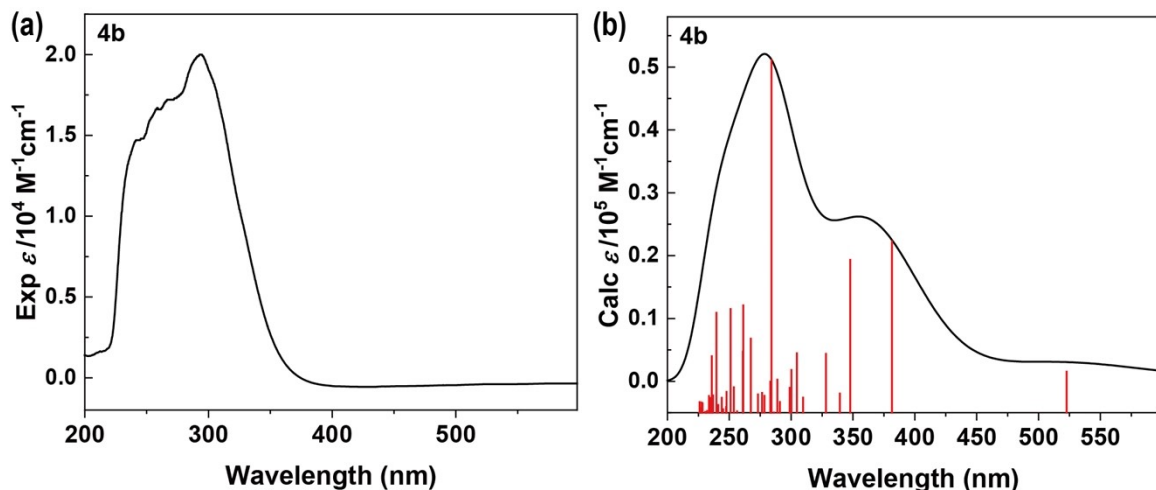


Figure S4. Computed, at the TD-DFT, B3LYP-D3/6-31g(d), level of theory and experimental UV-vis spectra of **4b**.

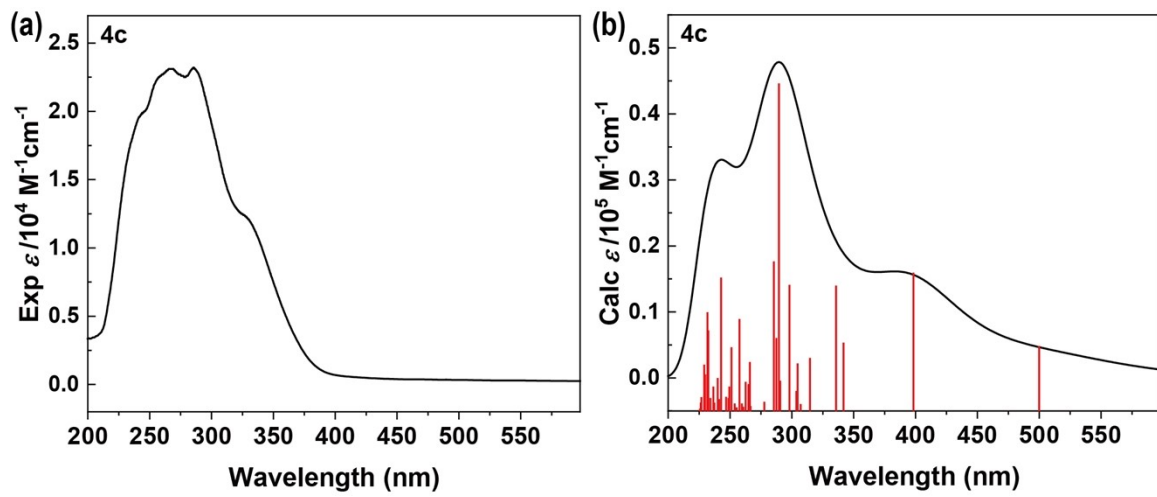


Figure S5. Computed, at the TD-DFT, B3LYP-D3/6-31g(d), level of theory and experimental UV-vis spectra of **4c**.

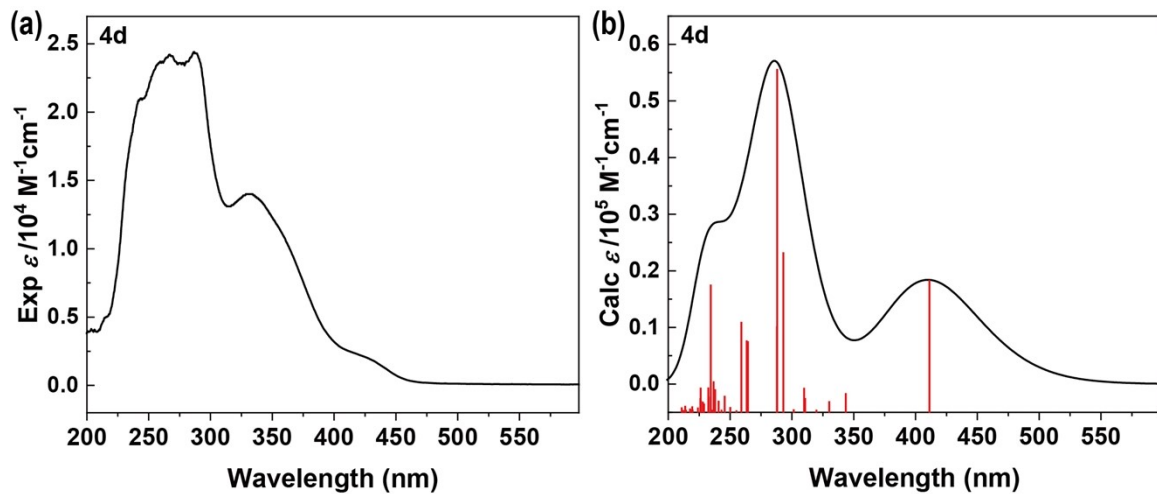


Figure S6. Computed, at the TD-DFT, B3LYP-D3/6-31g(d), level of theory and experimental UV-vis spectra of **4d**.

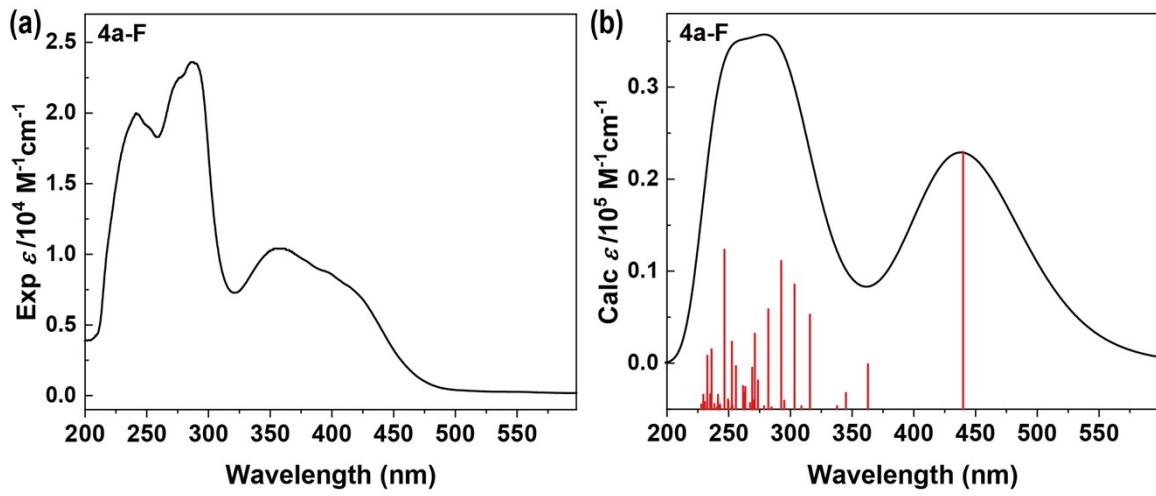


Figure S7. Computed, at the TD-DFT, B3LYP-D3/6-31g(d), level of theory and experimental UV-vis spectra of **4a-F**.

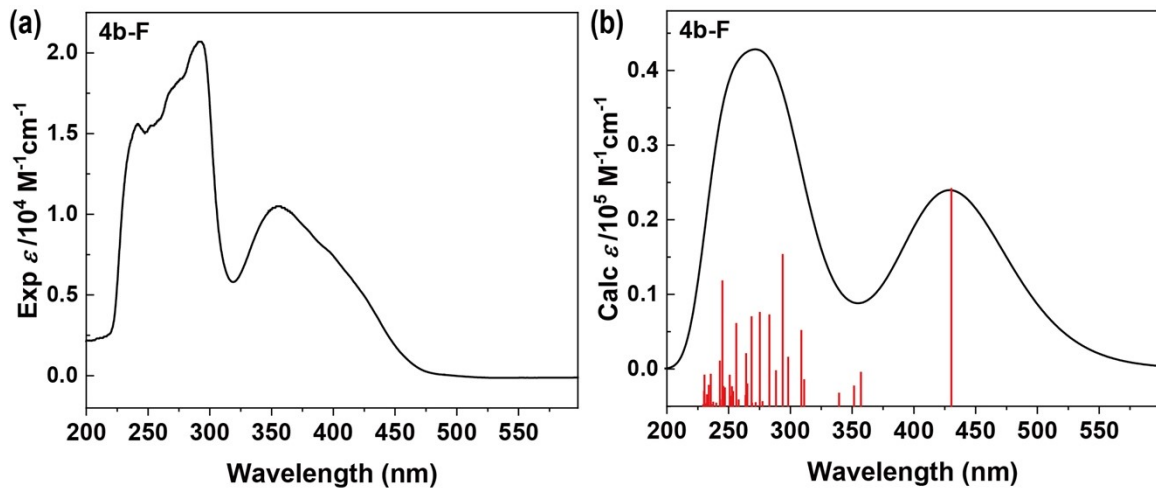


Figure S8. Computed, at the TD-DFT, B3LYP-D3/6-31g(d), level of theory and experimental UV-vis spectra of **4b-F**.

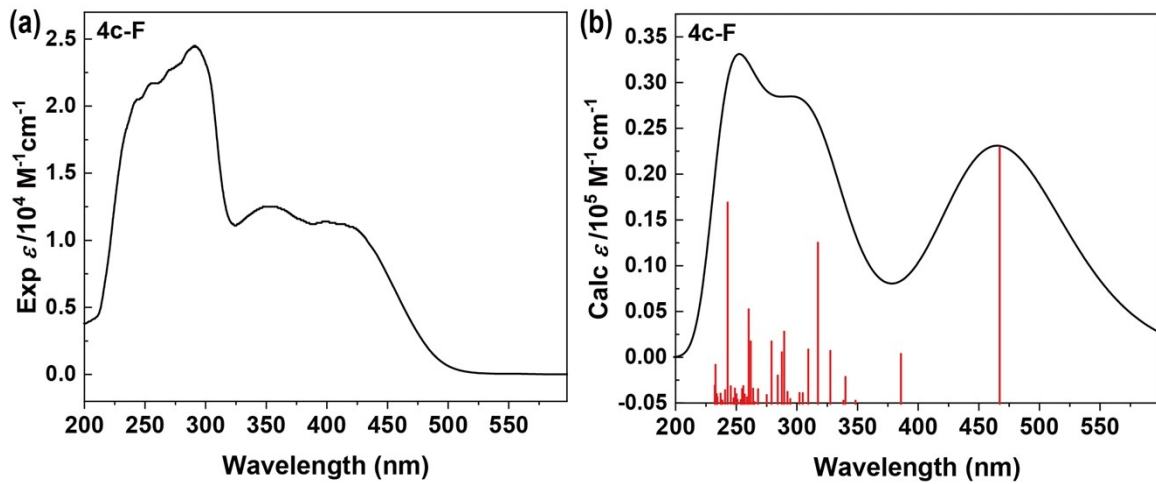


Figure S9. Computed, at the TD-DFT, B3LYP-D3/6-31g(d), level of theory and experimental UV-vis spectra of **4c-F**.

Table S1. Calculated ($\lambda_{\text{TD-DFT}}$) wavelengths of **4a**. Molecular orbitals (MOs) involved in the main electronic transition, f corresponds to the oscillator strength. (TD-DFT, B3LYP-D3/6-31g(d))

| $\lambda_{\text{TD-DFT}}$ | Oscillator Strength, f | MOs | |
|---------------------------|------------------------|-----------------------------|--------|
| 384.96 | 0.3482 | HOMO-1 \rightarrow LOMO | 16.36% |
| | | HOMO \rightarrow LOMO+1 | 67.91% |
| 344.42 | 0.2178 | HOMO-1 \rightarrow LOMO | 65.91% |
| | | HOMO \rightarrow LOMO+1 | 15.95% |
| | | HOMO \rightarrow LOMO+2 | 12.71% |
| 320.75 | 0.1074 | HOMO-3 \rightarrow LOMO | 18.44% |
| | | HOMO-2 \rightarrow LOMO | 59.67% |
| | | HOMO \rightarrow LOMO+2 | 27.34% |
| | | HOMO \rightarrow LOMO+3 | 12.03% |
| 298.02 | 0.1548 | HOMO-5 \rightarrow LOMO | 29.71% |
| | | HOMO-4 \rightarrow LOMO | 49.53% |
| | | HOMO-3 \rightarrow LOMO | 23.97% |
| | | HOMO-2 \rightarrow LOMO | 12.51% |
| | | HOMO \rightarrow LOMO+3 | 19.24% |
| | | HOMO \rightarrow LOMO+4 | 12.59% |
| 259.27 | 0.1467 | HOMO-10 \rightarrow LOMO | 11.86% |
| | | HOMO-8 \rightarrow LOMO | 27.38% |
| | | HOMO-2 \rightarrow LOMO+1 | 18.00% |

| | | | |
|--------|--------|-----------------|--------|
| | | HOMO ->LOMO+8 | 15.67% |
| | | HOMO ->LOMO+9 | 14.88% |
| | | HOMO ->LOMO+10 | 51.02% |
| 241.95 | 0.2265 | HOMO-8 ->LOMO | 10.78% |
| | | HOMO-2 ->LOMO+2 | 61.34% |
| | | HOMO-2 ->LOMO+3 | 15.89% |
| | | HOMO-1 ->LOMO+3 | 16.75% |
| 232.10 | 0.0958 | HOMO-8 ->LOMO+1 | 16.38% |
| | | HOMO-8 ->LOMO+2 | 11.53% |
| | | HOMO-7 ->LOMO+1 | 25.47% |
| | | HOMO-2 ->LOMO+3 | 15.35% |
| | | HOMO-2 ->LOMO+4 | 21.42% |
| | | HOMO-1 ->LOMO+3 | 22.26% |
| | | HOMO-1 ->LOMO+4 | 25.05% |
| | | HOMO-1 ->LOMO+5 | 26.47% |
| | | HOMO-1 ->LOMO+8 | 10.57% |
| | | HOMO ->LOMO+11 | 19.75% |

Table S2. Calculated ($\lambda_{\text{TD-DFT}}$) wavelengths of **4b**. Molecular orbitals (MOs) involved in the main electronic transition, f corresponds to the oscillator strength. (TD-DFT, B3LYP-D3/6-31g(d))

| $\lambda_{\text{TD-DFT}}$ | Oscillator Strength, f | MOs | |
|---------------------------|------------------------|-----------------|--------|
| 381.69 | 0.3731 | HOMO-1 ->LOMO | 18.37% |
| | | HOMO ->LOMO+1 | 67.26% |
| 348.08 | 0.2702 | HOMO-1 ->LOMO | 65.17% |
| | | HOMO ->LOMO+1 | 18.15% |
| | | HOMO ->LOMO+2 | 13.38% |
| 328.39 | 0.1042 | HOMO-2 ->LOMO | 29.32% |
| | | HOMO ->LOMO+2 | 59.14% |
| | | HOMO ->LOMO+3 | 15.72% |
| 304.90 | 0.1052 | HOMO-3 ->LOMO | 59.70% |
| | | HOMO ->LOMO+3 | 31.43% |
| 284.39 | 0.6227 | HOMO-6 ->LOMO | 10.37% |
| | | HOMO-5 ->LOMO | 13.23% |
| | | HOMO-1 ->LOMO+1 | 60.07% |
| | | HOMO ->LOMO+4 | 22.75% |
| | | HOMO ->LOMO+8 | 12.08% |
| 267.64 | 0.1308 | HOMO-7 ->LOMO | 11.68% |
| | | HOMO-2 ->LOMO+1 | 63.02% |
| | | HOMO ->LOMO+3 | 10.68% |
| | | HOMO ->LOMO+9 | 16.27% |
| 261.55 | 0.1897 | HOMO-10 ->LOMO | 18.91% |
| | | HOMO-1 ->LOMO+1 | 10.06% |
| | | HOMO ->LOMO+8 | 19.42% |
| | | HOMO ->LOMO+10 | 58.63% |
| 261.23 | 0.1078 | HOMO-10 ->LOMO | 18.17% |
| | | HOMO-2 ->LOMO+1 | 16.94% |
| | | HOMO-1 ->LOMO+2 | 19.93% |
| | | HOMO ->LOMO+8 | 15.20% |
| | | HOMO ->LOMO+9 | 56.46% |
| 251.33 | 0.1833 | HOMO-10 ->LOMO | 27.46% |
| | | HOMO-9 ->LOMO | 11.38% |
| | | HOMO-8 ->LOMO | 27.01% |
| | | HOMO-3 ->LOMO+1 | 10.15% |
| | | HOMO-2 ->LOMO+2 | 49.81% |
| | | HOMO ->LOMO+10 | 13.64% |

Table S3. Calculated ($\lambda_{\text{TD-DFT}}$) wavelengths of **4c**. Molecular orbitals (MOs) involved in the main electronic transition, f corresponds to the oscillator strength. (TD-DFT, B3LYP-D3/6-31g(d))

| $\lambda_{\text{TD-DFT}}$ | Oscillator Strength, f | MOs | |
|---------------------------|------------------------|-----------------|--------|
| 397.96 | 0.3393 | HOMO-1 ->LOMO | 13.10% |
| | | HOMO ->LOMO+1 | 68.29% |
| 341.40 | 0.0926 | HOMO-1 ->LOMO | 43.94% |
| | | HOMO ->LOMO+1 | 10.83% |
| | | HOMO ->LOMO+2 | 50.11% |
| | | HOMO ->LOMO+3 | 12.61% |
| 335.41 | 0.1719 | HOMO-1 ->LOMO | 51.03% |
| | | HOMO ->LOMO+2 | 45.08% |
| 297.77 | 0.1729 | HOMO-5 ->LOMO | 50.31% |
| | | HOMO-4 ->LOMO | 42.46% |
| | | HOMO-2 ->LOMO | 15.84% |
| 289.25 | 0.4525 | HOMO-1 ->LOMO+1 | 52.83% |
| | | HOMO ->LOMO+4 | 25.73% |
| | | HOMO ->LOMO+8 | 26.68% |
| | | HOMO ->LOMO+9 | 14.36% |
| | | HOMO ->LOMO+10 | 13.22% |
| 285.24 | 0.2054 | HOMO-1 ->LOMO+1 | 25.90% |
| | | HOMO ->LOMO+4 | 25.57% |
| | | HOMO ->LOMO+5 | 12.02% |
| | | HOMO ->LOMO+7 | 16.28% |
| | | HOMO ->LOMO+8 | 45.26% |
| | | HOMO ->LOMO+9 | 22.35% |
| | | HOMO ->LOMO+10 | 19.91% |
| 257.39 | 0.1254 | HOMO-8 ->LOMO | 14.15% |
| | | HOMO-3 ->LOMO+1 | 14.09% |
| | | HOMO ->LOMO+8 | 28.47% |
| | | HOMO ->LOMO+9 | 10.56% |
| | | HOMO ->LOMO+10 | 55.01% |
| 232.23 | 0.1095 | HOMO-11 ->LOMO | 22.59% |
| | | HOMO-9 ->LOMO | 11.65% |
| | | HOMO-7 ->LOMO+1 | 14.92% |
| | | HOMO-4 ->LOMO+2 | 55.30% |
| | | HOMO-1 ->LOMO+3 | 15.74% |

Table S4. Calculated ($\lambda_{\text{TD-DFT}}$) wavelengths of **4d**. Molecular orbitals (MOs) involved in the main electronic transition, f corresponds to the oscillator strength. (TD-DFT, B3LYP-D3/6-31g(d))

| $\lambda_{\text{TD-DFT}}$ | Oscillator Strength, f | MOs | |
|---------------------------|------------------------|-----------------|--------|
| 410.94 | 0.4496 | HOMO ->LOMO | 69.69% |
| 292.71 | 0.3280 | HOMO-1 ->LOMO | 34.75% |
| | | HOMO ->LOMO+5 | 24.70% |
| | | HOMO ->LOMO+6 | 15.46% |
| | | HOMO ->LOMO+7 | 28.07% |
| | | HOMO ->LOMO+8 | 32.57% |
| | | HOMO ->LOMO+9 | 26.59% |
| | | HOMO ->LOMO+10 | 10.45% |
| 287.73 | 0.7070 | HOMO-1 ->LOMO | 42.65% |
| | | HOMO ->LOMO+5 | 23.40% |
| | | HOMO ->LOMO+6 | 28.69% |
| | | HOMO ->LOMO+8 | 32.99% |
| | | HOMO ->LOMO+9 | 22.37% |
| 287.68 | 0.1750 | HOMO-1 ->LOMO | 20.00% |
| | | HOMO ->LOMO+7 | 62.54% |
| | | HOMO ->LOMO+8 | 15.37% |
| | | HOMO ->LOMO+9 | 13.54% |
| 264.11 | 0.1440 | HOMO-2 ->LOMO | 34.22% |
| | | HOMO ->LOMO+8 | 34.15% |
| | | HOMO ->LOMO+9 | 46.32% |
| 263.11 | 0.1457 | HOMO-2 ->LOMO | 50.95% |
| | | HOMO ->LOMO+8 | 20.60% |
| | | HOMO ->LOMO+9 | 19.30% |
| | | HOMO ->LOMO+10 | 32.70% |
| 258.84 | 0.1841 | HOMO-6 ->LOMO | 13.65% |
| | | HOMO-2 ->LOMO | 29.12% |
| | | HOMO-1 ->LOMO+2 | 12.22% |
| | | HOMO ->LOMO+9 | 18.19% |
| | | HOMO ->LOMO+10 | 54.48% |
| 234.14 | 0.2610 | HOMO-3 ->LOMO | 18.70% |
| | | HOMO-2 ->LOMO+2 | 60.76% |
| | | HOMO-1 ->LOMO+5 | 20.89% |
| | | HOMO ->LOMO+11 | 10.63% |

Table S5. Calculated ($\lambda_{\text{TD-DFT}}$) wavelengths of **4a-F**. Molecular orbitals (MOs) involved in the main electronic transition, f corresponds to the oscillator strength. (TD-DFT, B3LYP-D3/6-31g(d))

| $\lambda_{\text{TD-DFT}}$ | Oscillator Strength, f | MOs | |
|---------------------------|------------------------|------------------|--------|
| 444.11 | 0.4133 | HOMO ->LOMO | 69.42% |
| 378.56 | 0.1029 | HOMO ->LOMO+1 | 69.19% |
| 300.91 | 0.2392 | HOMO-4 ->LOMO | 35.51% |
| | | HOMO-3 ->LOMO | 44.09% |
| | | HOMO-2 ->LOMO | 24.15% |
| | | HOMO-1 ->LOMO | 15.22% |
| | | HOMO ->LOMO+8 | 24.78% |
| | | HOMO-4 ->LOMO | 31.73% |
| 282.27 | 0.1763 | HOMO ->LOMO+7 | 21.57% |
| | | HOMO ->LOMO+8 | 56.38% |
| | | HOMO-6 ->LOMO | 65.74% |
| 267.13 | 0.1722 | HOMO ->LOMO+10 | 11.58% |
| | | HOMO ->LOMO+11 | 12.48% |
| | | HOMO-6 ->LOMO+1 | 63.82% |
| 253.28 | 0.3580 | HOMO-4 ->LOMO+2 | 13.77% |
| | | HOMO-3 ->LOMO+3 | 11.48% |
| | | HOMO-1 ->LOMO+4 | 14.38% |
| | | HOMO-6 ->LOMO+1 | 12.09% |
| 252.64 | 0.0174 | HOMO-4 ->LOMO+3 | 43.97% |
| | | HOMO-3 ->LOMO+2 | 10.28% |
| | | HOMO-3 ->LOMO+3 | 51.31% |
| | | HOMO-8 ->LOMO | 14.26% |
| 251.30 | 0.0158 | HOMO-6 ->LOMO+1 | 10.68% |
| | | HOMO-6 ->LOMO+2 | 16.88% |
| | | HOMO-1 ->LOMO+4 | 59.63% |
| | | HOMO-11 ->LOMO | 16.25% |
| 249.96 | 0.0194 | HOMO-11 ->LOMO+1 | 13.20% |
| | | HOMO-9 ->LOMO+2 | 12.13% |
| | | HOMO-6 ->LOMO+1 | 12.78% |
| | | HOMO-6 ->LOMO+2 | 49.26% |
| | | HOMO-6 ->LOMO+3 | 12.38% |
| | | HOMO-5 ->LOMO+2 | 13.92% |
| | | HOMO-4 ->LOMO+2 | 28.58% |
| | | HOMO-1 ->LOMO+4 | 16.47% |

Table S6. Calculated ($\lambda_{\text{TD-DFT}}$) wavelengths of **4b-F**. Molecular orbitals (MOs) involved in the main electronic transition, f corresponds to the oscillator strength. (TD-DFT, B3LYP-D3/6-31g(d))

| $\lambda_{\text{TD-DFT}}$ | Oscillator Strength, f | MOs | |
|---------------------------|------------------------|-----------------|--------|
| 430.55 | 0.5816 | HOMO ->LOMO | 69.91% |
| 309.09 | 0.1320 | HOMO-2 ->LOMO | 10.16% |
| | | HOMO-1 ->LOMO | 50.63% |
| | | HOMO ->LOMO+5 | 22.89% |
| | | HOMO ->LOMO+6 | 35.31% |
| | | HOMO ->LOMO+7 | 15.53% |
| 293.97 | 0.2665 | HOMO-2 ->LOMO | 29.01% |
| | | HOMO-1 ->LOMO | 14.43% |
| | | HOMO ->LOMO+4 | 55.54% |
| | | HOMO ->LOMO+5 | 17.86% |
| | | HOMO ->LOMO+6 | 17.02% |
| 283.29 | 0.1595 | HOMO-5 ->LOMO | 10.84% |
| | | HOMO-3 ->LOMO | 18.44% |
| | | HOMO-2 ->LOMO | 14.69% |
| | | HOMO ->LOMO+5 | 51.01% |
| | | HOMO ->LOMO+6 | 34.76% |
| | | HOMO ->LOMO+7 | 16.30% |
| 275.58 | 0.1641 | HOMO-4 ->LOMO | 28.89% |
| | | HOMO-1 ->LOMO+1 | 23.62% |
| | | HOMO ->LOMO+6 | 19.25% |
| | | HOMO ->LOMO+7 | 51.10% |
| 268.82 | 0.1561 | HOMO-7 ->LOMO | 20.66% |
| | | HOMO-5 ->LOMO | 60.65% |
| | | HOMO-1 ->LOMO+2 | 19.90% |
| 256.46 | 0.1445 | HOMO-7 ->LOMO | 21.29% |
| | | HOMO-3 ->LOMO+1 | 38.80% |
| 245.21 | 0.2197 | HOMO-5 ->LOMO+1 | 56.60% |
| | | HOMO-5 ->LOMO+2 | 15.18% |
| | | HOMO-3 ->LOMO+2 | 24.33% |
| | | HOMO-3 ->LOMO+3 | 12.48% |
| | | HOMO-2 ->LOMO+2 | 10.76% |
| | | HOMO-2 ->LOMO+3 | 16.35% |

Table S7. Calculated ($\lambda_{\text{TD-DFT}}$) wavelengths of **4c-F**. Molecular orbitals (MOs) involved in the main electronic transition, f corresponds to the oscillator strength. (TD-DFT, B3LYP-D3/6-31g(d))

| $\lambda_{\text{TD-DFT}}$ | Oscillator Strength, f | MOs | |
|---------------------------|------------------------|-----------------|--------|
| 467.46 | 0.5582 | HOMO ->LOMO | 70.06% |
| 317.61 | 0.2685 | HOMO-3 ->LOMO | 67.31% |
| | | HOMO ->LOMO+3 | 10.65% |
| 309.61 | 0.0905 | HOMO-5 ->LOMO | 10.54% |
| | | HOMO-4 ->LOMO | 67.41% |
| 289.77 | 0.1200 | HOMO-6 ->LOMO | 11.81% |
| | | HOMO-1 ->LOMO+1 | 27.11% |
| | | HOMO ->LOMO+4 | 53.75% |
| | | HOMO ->LOMO+5 | 11.92% |
| | | HOMO ->LOMO+6 | 26.02% |
| 287.82 | 0.0856 | HOMO-7 ->LOMO | 14.20% |
| | | HOMO-6 ->LOMO | 64.22% |
| | | HOMO-3 ->LOMO+1 | 20.64% |
| | | HOMO ->LOMO+4 | 10.28% |
| 279.26 | 0.1038 | HOMO-4 ->LOMO+1 | 13.95% |
| | | HOMO-3 ->LOMO+1 | 33.61% |
| | | HOMO ->LOMO+5 | 46.00% |
| | | HOMO ->LOMO+6 | 33.09% |
| 262.15 | 0.1038 | HOMO-7 ->LOMO | 53.47% |
| | | HOMO-6 ->LOMO | 12.05% |
| | | HOMO-6 ->LOMO+1 | 33.30% |
| | | HOMO-3 ->LOMO+3 | 13.24% |
| | | HOMO-1 ->LOMO+2 | 11.88% |
| 260.48 | 0.1574 | HOMO-7 ->LOMO | 28.63% |
| | | HOMO-6 ->LOMO+1 | 56.62% |
| | | HOMO-1 ->LOMO+2 | 13.26% |
| | | HOMO ->LOMO+8 | 18.70% |

4. Aggregation-induced fluorescence properties

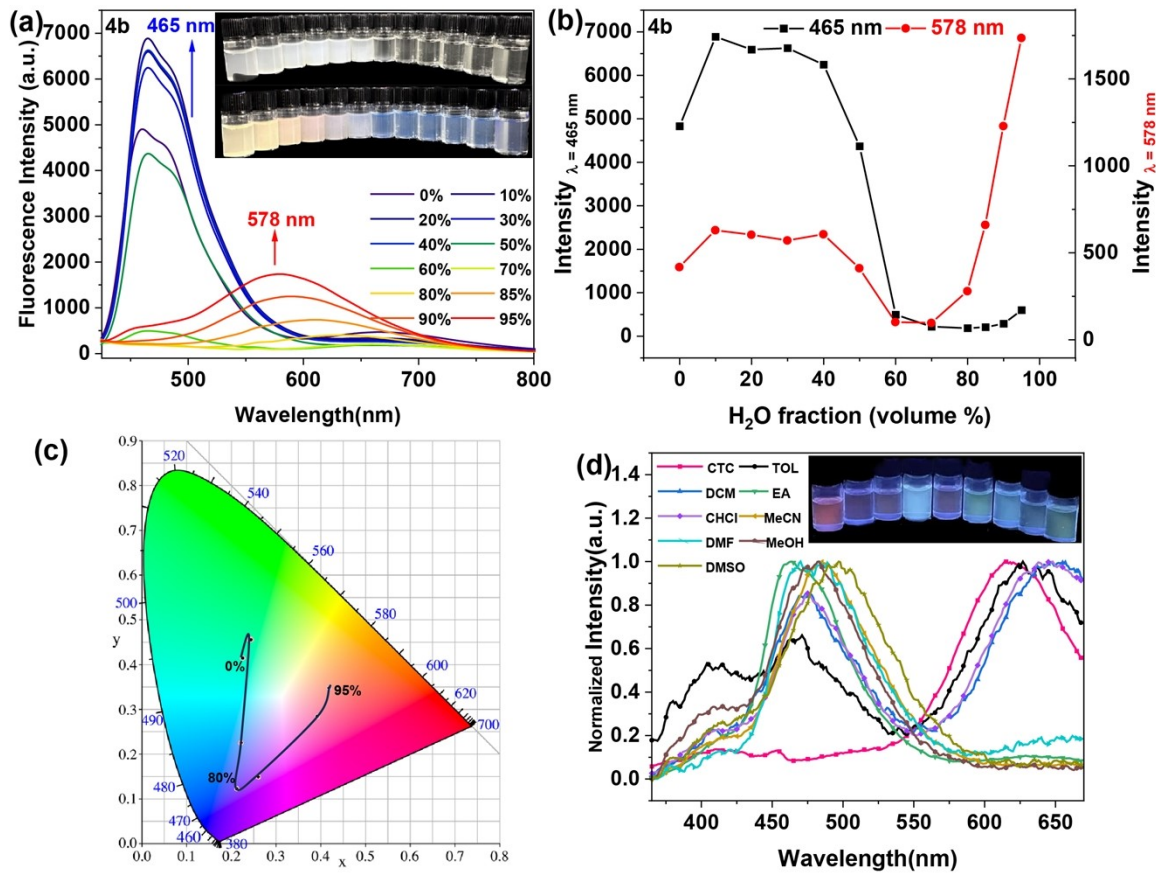


Figure S10. Photoluminescence (PL) spectra of **4b** in different THF/water ratios. (a) Photographs of aggregates under UV light, $\lambda_{\text{ex}} = 365 \text{ nm}$. (b) Emission intensity of **4b** as the THF/water ratio is altered (Left: fluorescence intensity at 465 nm; Right: fluorescence intensity at 578 nm). (c) CIE chromaticity. (d) Emission spectra of **4b** in solutions (with different polarities).

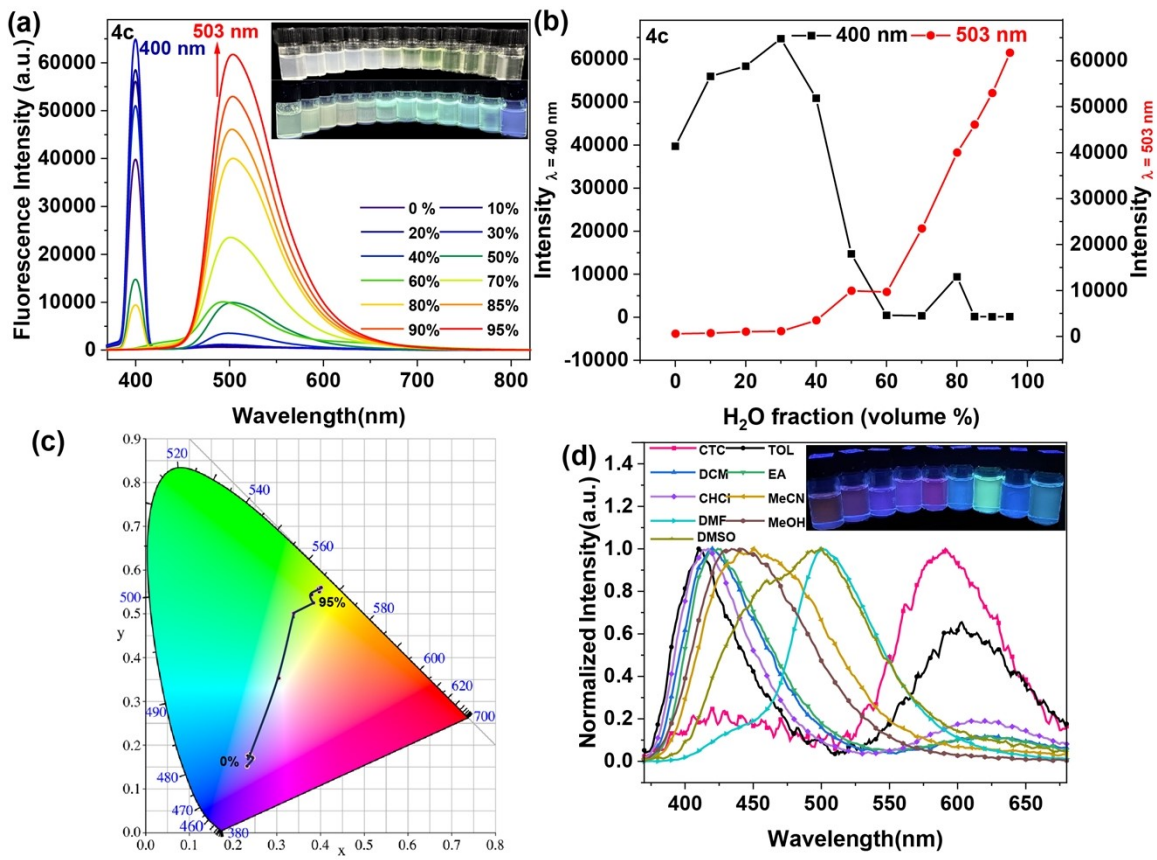


Figure S11. Photoluminescence (PL) spectra of **4c** in different THF/water ratios. (a) Photographs of aggregates under UV light, $\lambda_{\text{ex}} = 365 \text{ nm}$. (b) Emission intensity of **4c** as the THF/water ratio is altered (Left: fluorescence intensity at 400 nm; Right: fluorescence intensity at 503 nm). (c) CIE chromaticity. (d) Emission spectra of **4c** in solutions (with different polarities).

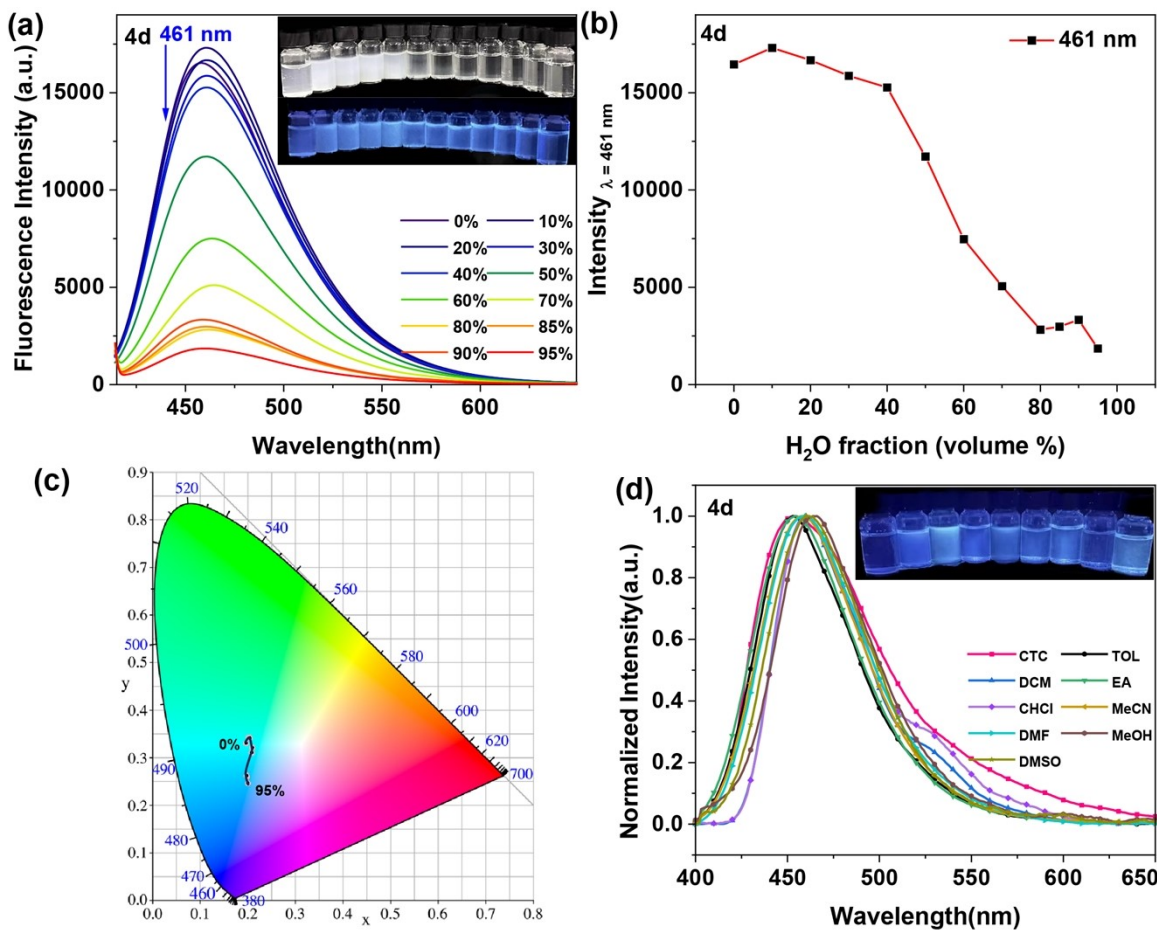


Figure S12. Photoluminescence (PL) spectra of **4d** in different THF/water ratios. (a) Photographs of aggregates under UV light, $\lambda_{ex} = 365$ nm. (b) Emission intensity of **4d** as the THF/water ratio is altered (Left: fluorescence intensity at 465 nm; Right: fluorescence intensity at 578 nm). (c) CIE chromaticity. (d) Emission spectra of **4d** in solutions (with different polarities).

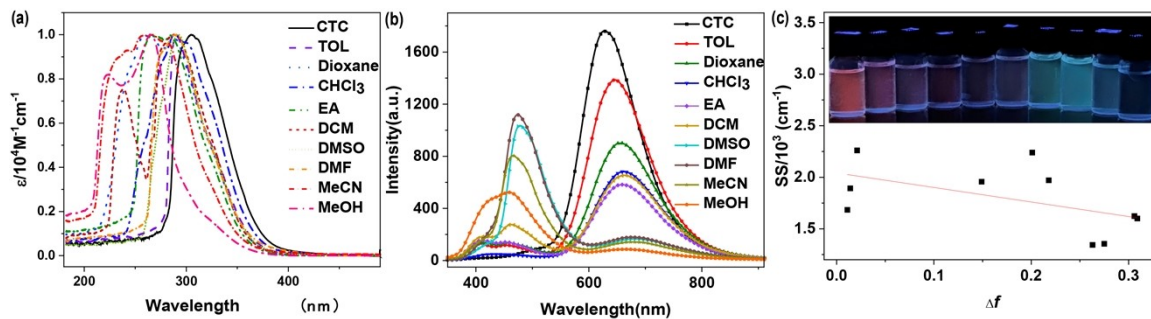


Figure S13. Figure Sx. (a) absorption and (b) emission spectra of 4a in different solvents; (c) Plots of Stokes shift (SS) of 4a versus solvent polarity parameter (Δf).

Table S8. Photophysical Properties of **4a** in Different Solvents

| Solvent | Δf^a | λ_{ab} (nm) ^b | λ_{em} (nm) ^c | SS ^d |
|------------------|--------------|----------------------------------|----------------------------------|-----------------|
| CCl ₄ | 0.011 | 305 | 627 | 1684 |
| Toluene | 0.014 | 290 | 643 | 1893 |
| dioxane | 0.021 | 264 | 655 | 2261 |
| chloroform | 0.149 | 288 | 660 | 1957 |
| EA | 0.201 | 266 | 658 | 2240 |
| DCM | 0.218 | 287 | 661 | 1971 |
| DMSO | 0.263 | 291 | 478 | 1344 |
| DMF | 0.275 | 289 | 475 | 1355 |
| acetonitrile | 0.306 | 265 | 465 | 1623 |
| Methanol | 0.309 | 265 | 460 | 1600 |

^a solvent polarity parameter taken from the Lippert-Mataga equation. ^b The longest λ_{max} values in the UV-Vis spectra. ^c Emission maxima in solvent. ^d Stokes shift = $1/\lambda_{abs} - 1/\lambda_{em}$.

5. Electrochemical properties

Cyclic voltammograms were recorded with a Metrohm PGSTAT204 electrochemical analyzer using DCM. The CV cell consisted of a gold electrode, a Pt wire counter electrode, and an Ag/AgCl reference electrode. All measurements were performed using DCM solutions of samples with a concentration of 1 mM and 0.1 M $\text{Bu}_4\text{N}^+\text{BF}_6^-$ as a supporting electrolyte with a scan rate of 100 mVs⁻¹. Potentials are determined against a ferrocene/ferrocenyl ion couple (Fc/Fc^+).

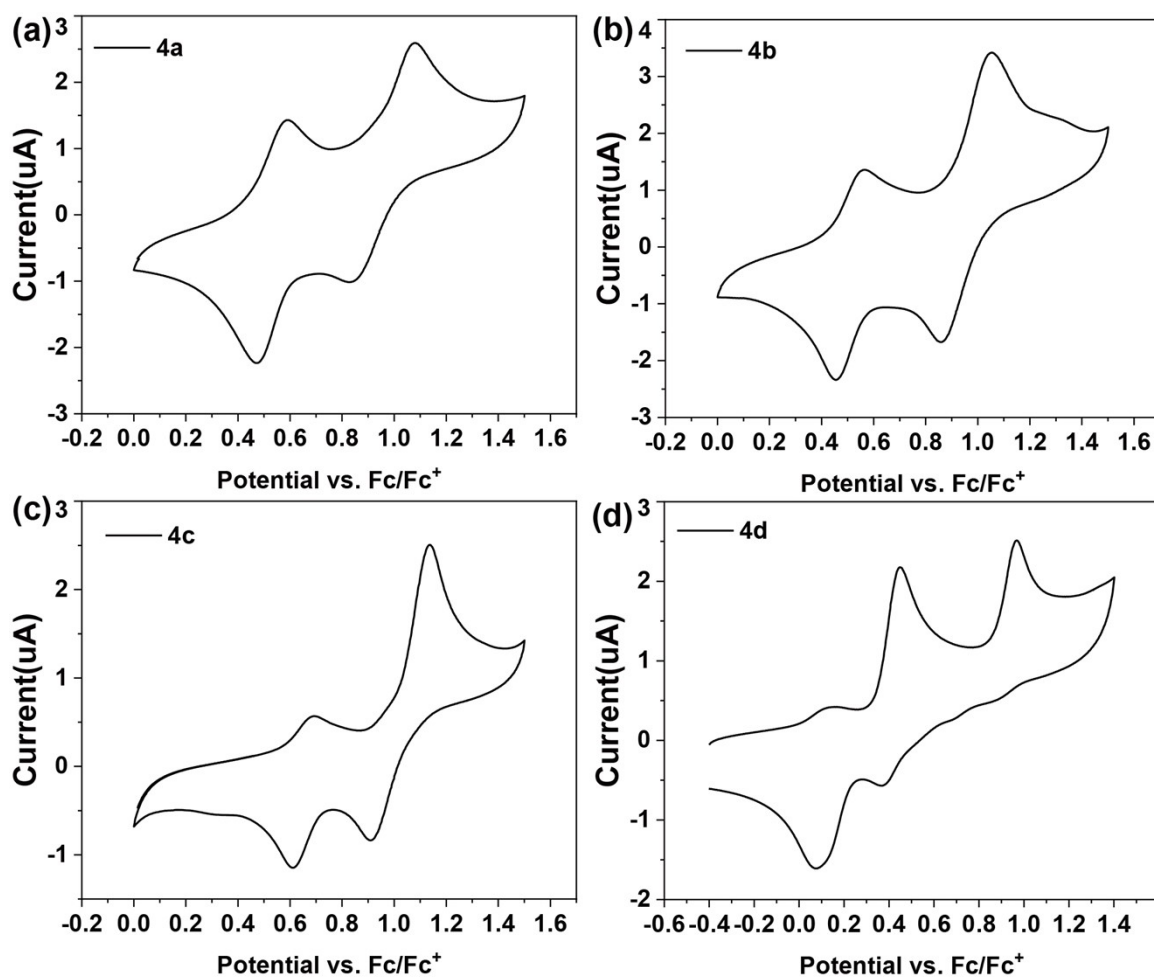


Figure S14. Cyclic voltammograms of **4a**, **4b**, **4c** and **4d** in DCM with $\text{Bu}_4\text{N}^+\text{BF}_6^-$ (0.1 M) as a supporting electrolyte, Fc = ferrocene.

6. Comparison of HOMO/LUMO plots

Table S9. Electronic properties of **4a**, **4b**, **4c** and **4d**

| Entry | E_g^a (eV) | E_{ox}^b (V) | HOMO(eV) (Exp) ^c | LUMO(eV) (Exp) ^d | HOMO(eV) (Cal) ^e | LUMO(eV) (Cal) ^e | E_g (eV) (Cal) ^e |
|-----------|--------------|----------------|--------------------------------|--------------------------------|--------------------------------|--------------------------------|----------------------------------|
| 4a | 3.59 | 0.79 | -5.59 | -2.00 | -5.40 | -0.95 | 4.46 |
| 4b | 3.55 | 0.86 | -5.66 | -2.11 | -5.30 | -0.85 | 4.45 |
| 4c | 3.40 | 0.96 | -5.76 | -2.36 | -5.74 | -1.45 | 4.29 |
| 4d | 3.20 | 0.78 | -5.58 | -2.38 | -4.88 | -0.79 | 4.09 |

^a E_g estimated from the UV-Vis absorption spectra.

^b Oxidation onset potentials measured by cyclic voltammetry.

^c HOMO = -(E_{OX} + 4.8) eV.

^d LUMO = HOMO + E_g .

^eTheoretical calculations have been carried out by using the GAUSSIAN09 suite of programs in gas-phase at the B3LYP/6-31G(d) levele,⁵ respectively.

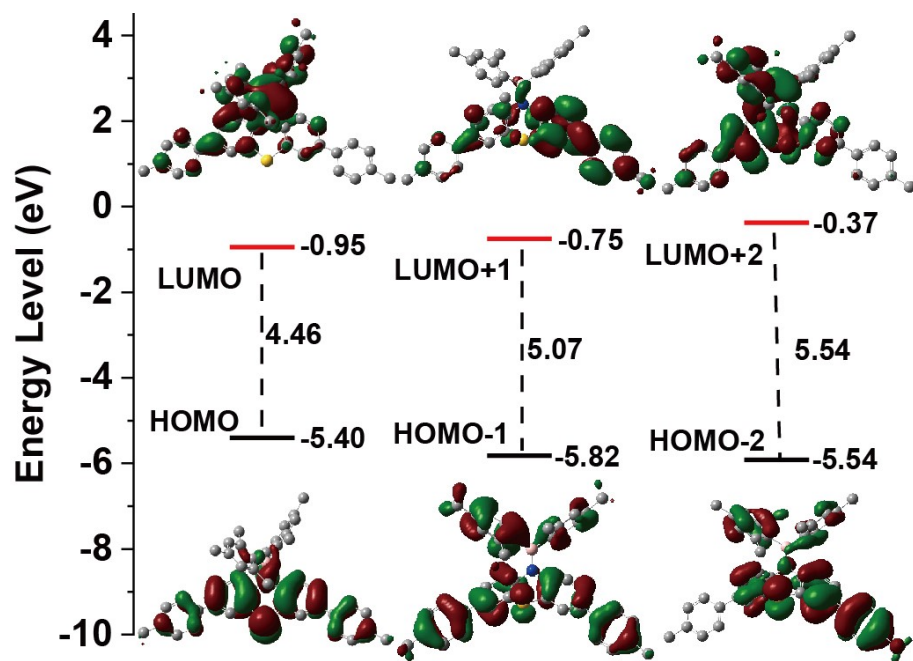


Figure S15. Computed molecular orbital plots for 4a.

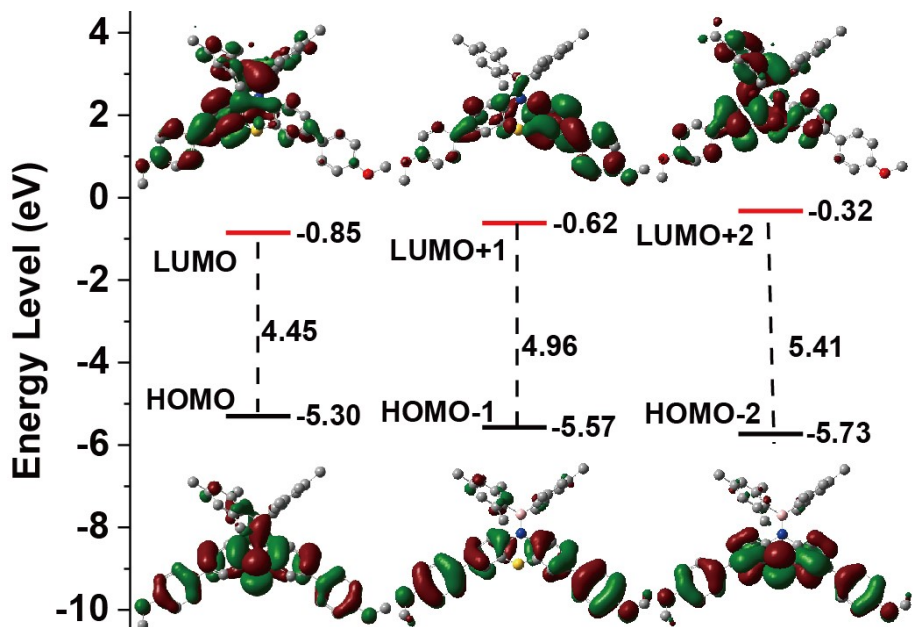


Figure S16. Computed molecular orbital plots for 4b.

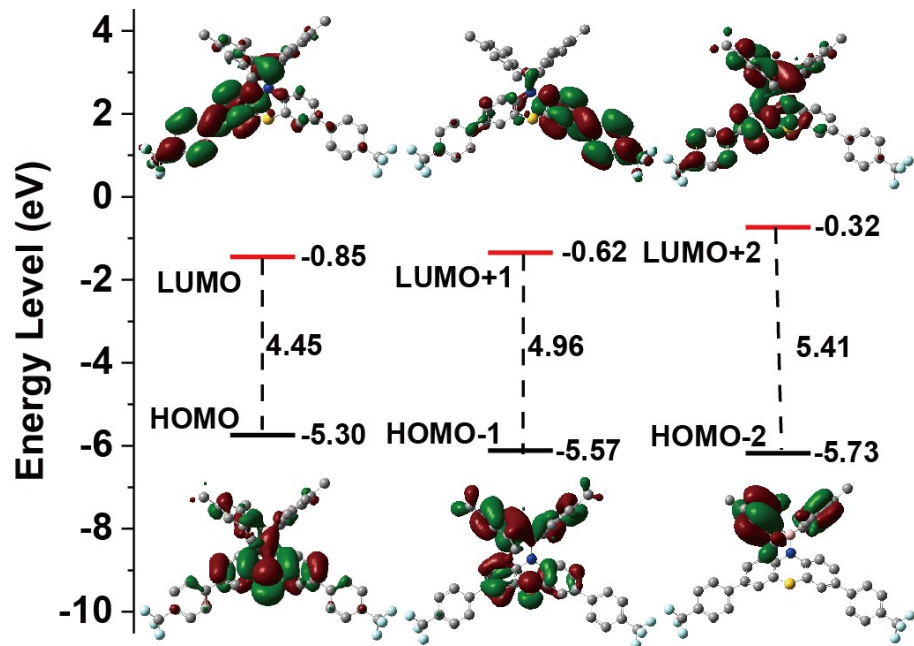


Figure S17. Computed molecular orbital plots for 4c.

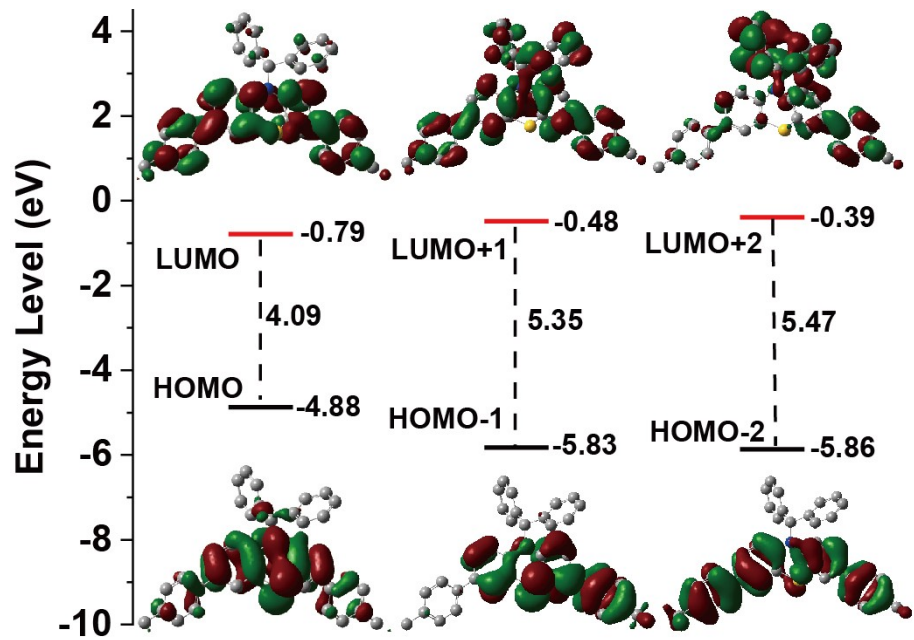


Figure S18. Computed molecular orbital plots for 4d.

7. Determination of the detection limit

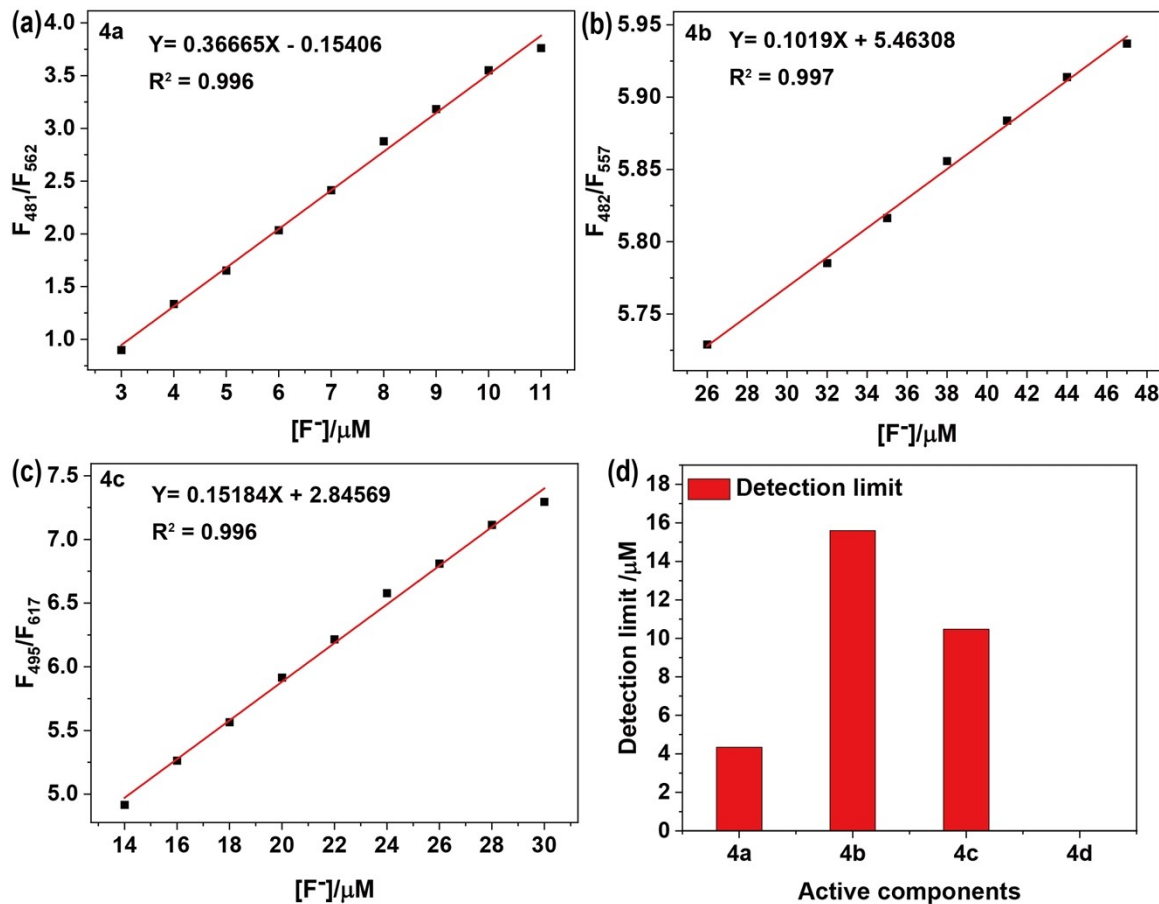


Figure S19. (a-c) The calibration curves and linear equation of **4a-4c** for FL intensity ratio changes upon gradual addition of F^- . (d)The calculated detection limits of **4a**, **4b**, and **4c**.

8. Reversibility of the MFC performance

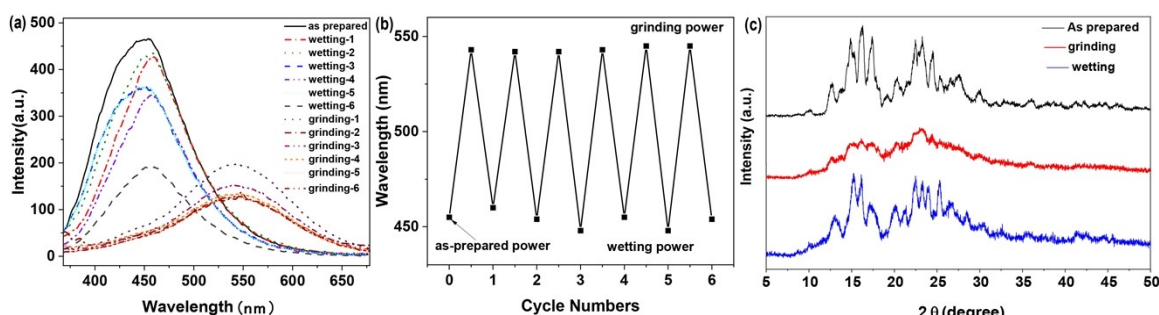
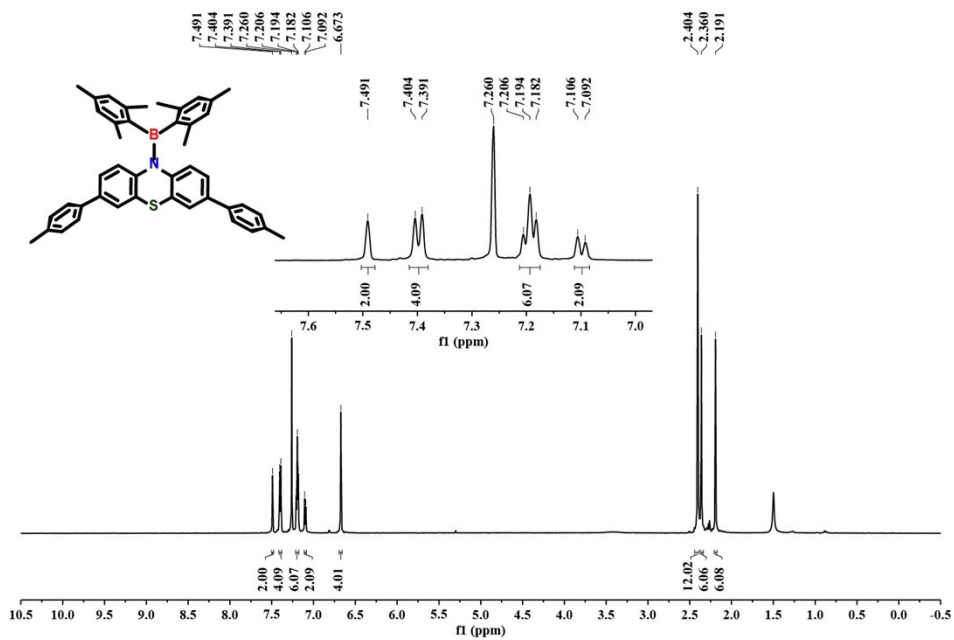
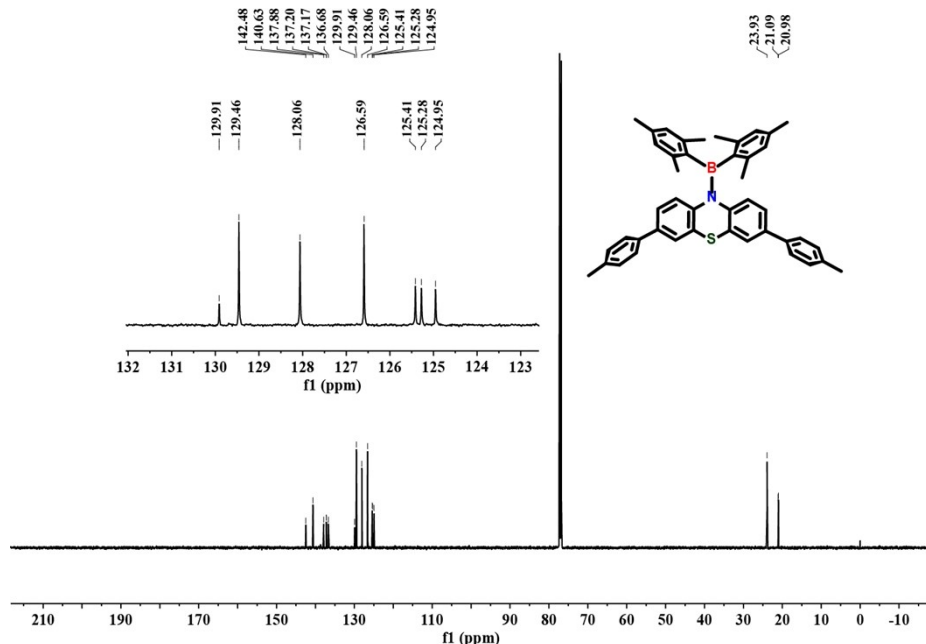


Figure S20. Emission spectra (a) and maximum emission wavelengths of **4a** upon repeating treated by grinding and wetting with DCM. (c) XRD patterns of **4a**: as-prepared, grinding and wetted samples.

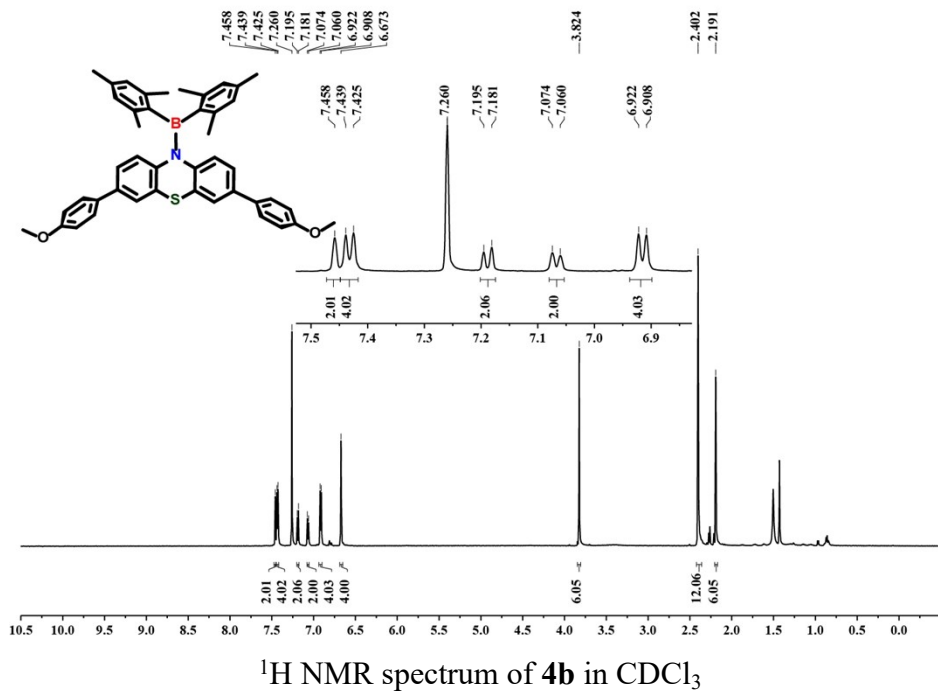
9. ^1H NMR and ^{13}C NMR spectra



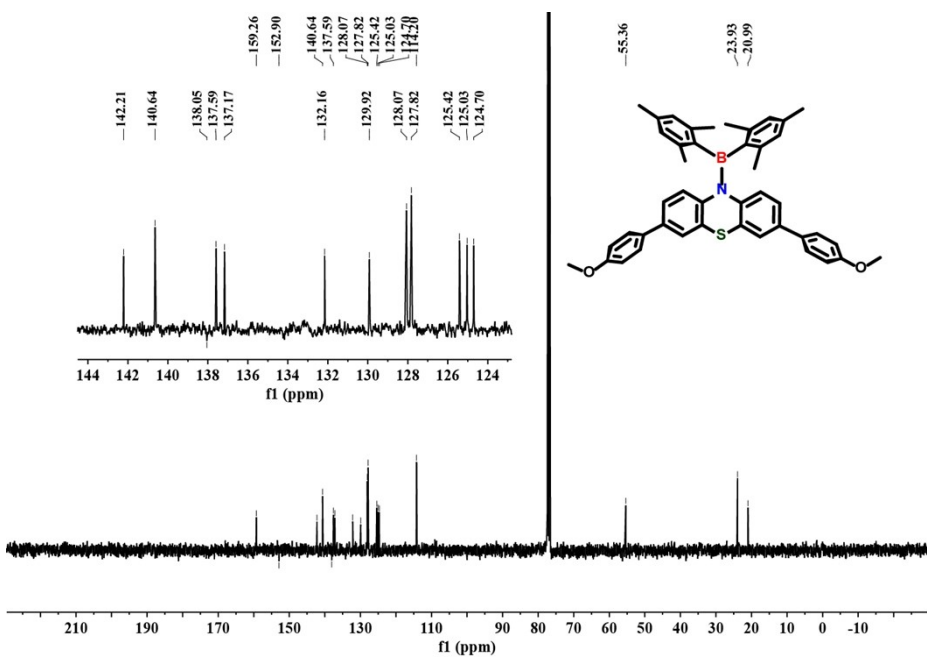
¹H NMR spectrum of **4a** in CDCl₃



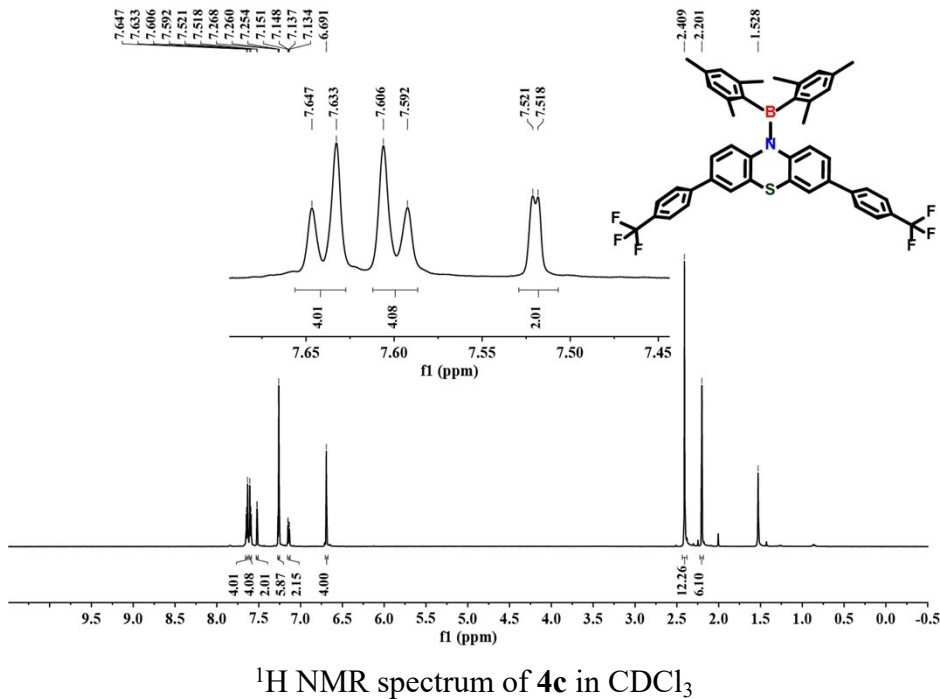
¹³C NMR spectrum of **4a** in CDCl₃



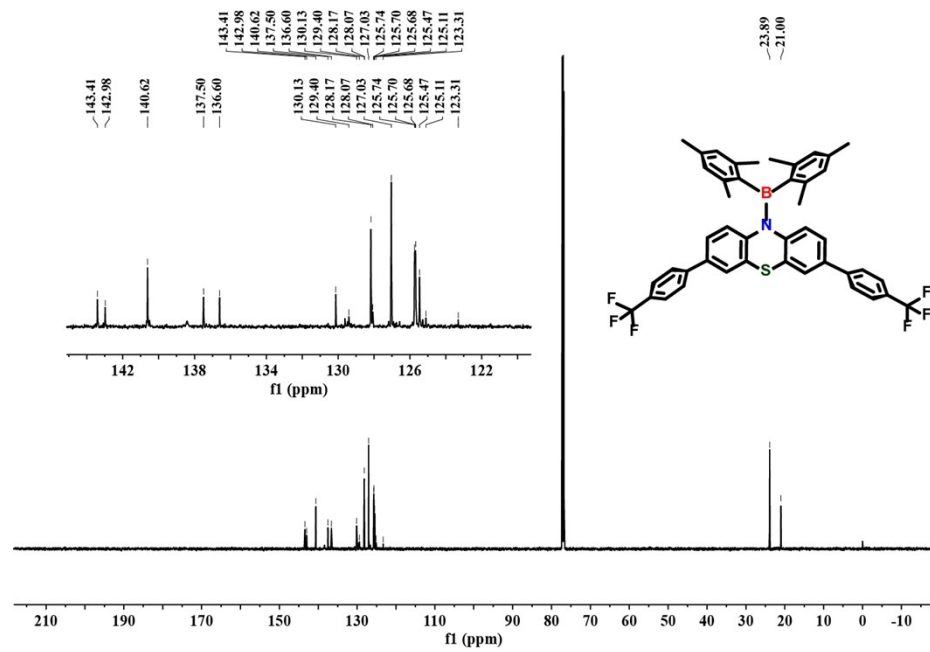
¹H NMR spectrum of **4b** in CDCl₃



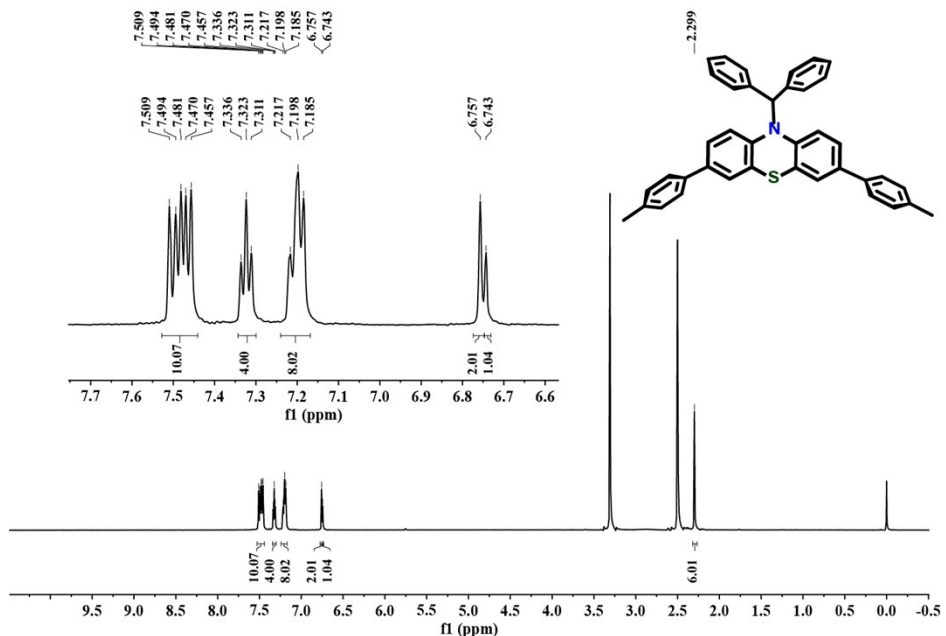
¹³C NMR spectrum of **4b** in CDCl₃



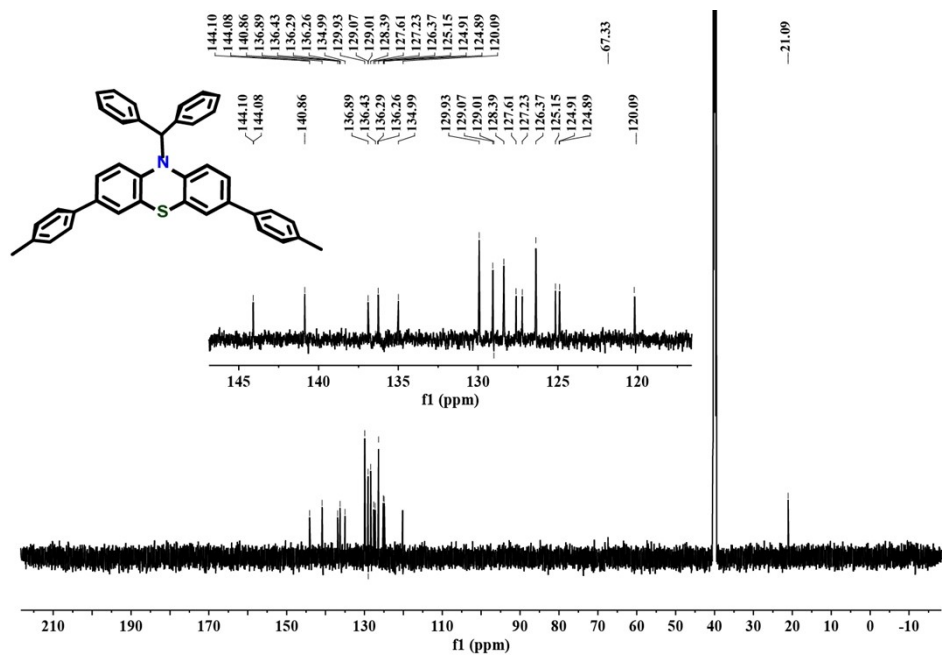
¹H NMR spectrum of **4c** in CDCl₃



¹³C NMR spectrum of **4c** in CDCl₃

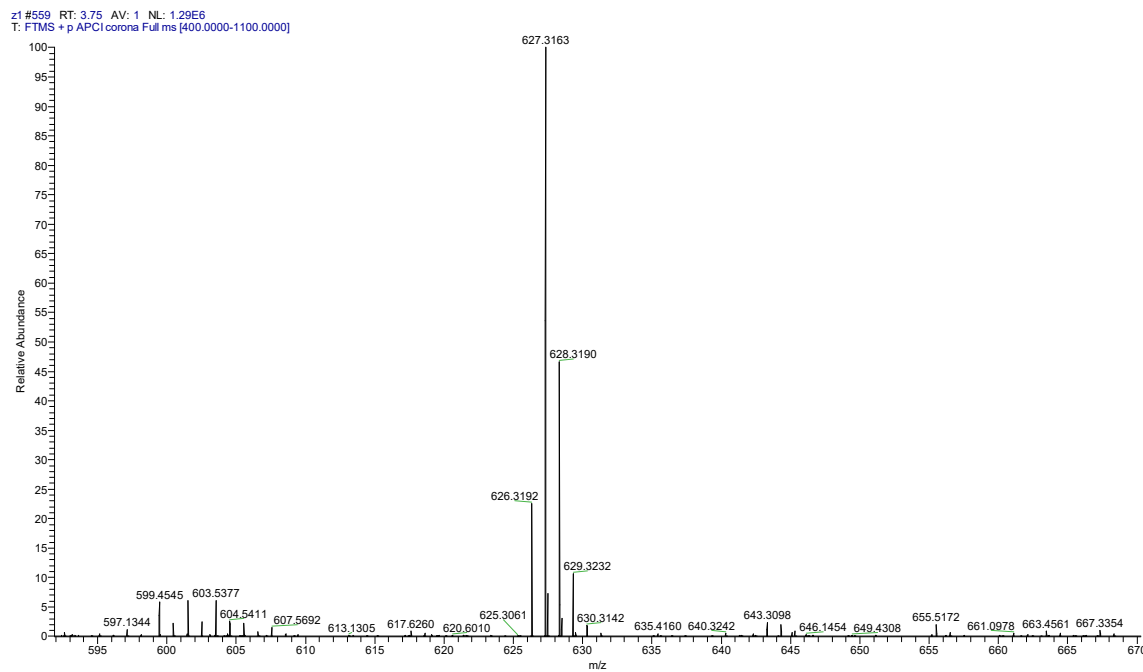


¹H NMR spectrum of **4d** in DMSO

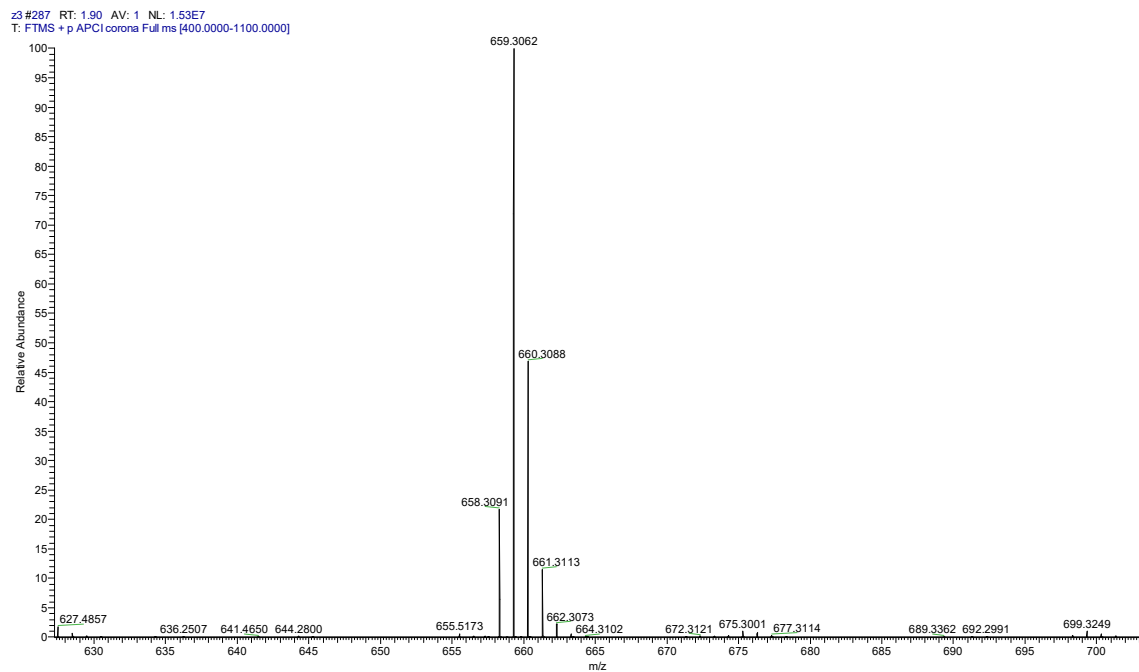


¹³C NMR spectrum of **4d** in DMSO

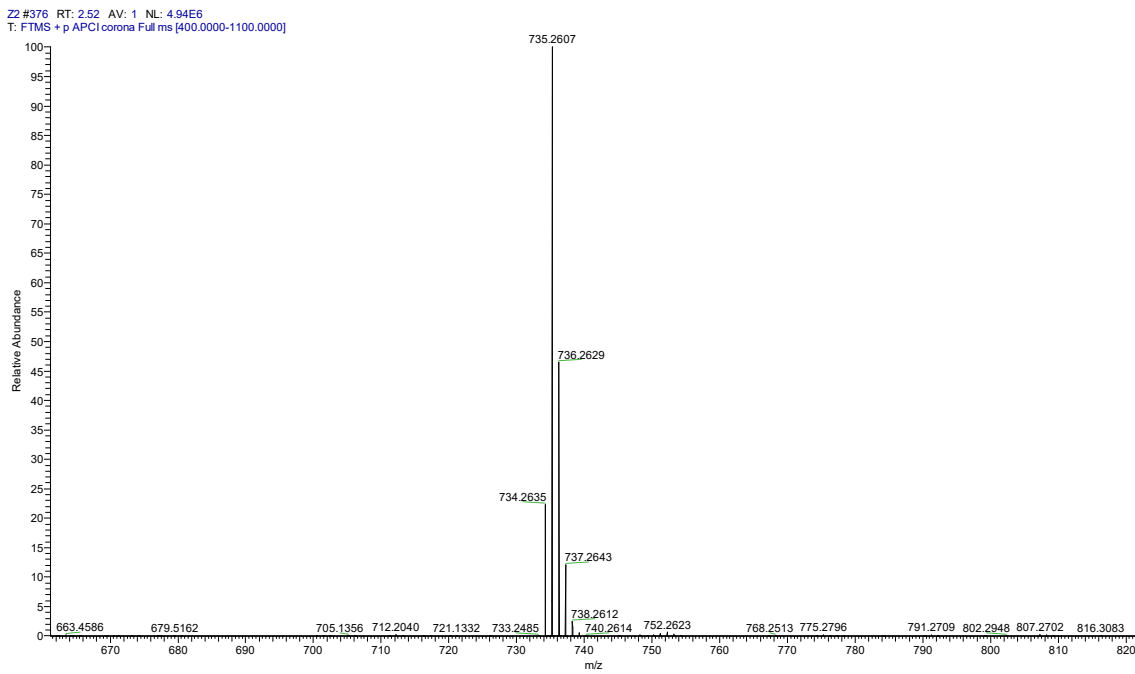
10. HRMS spectra



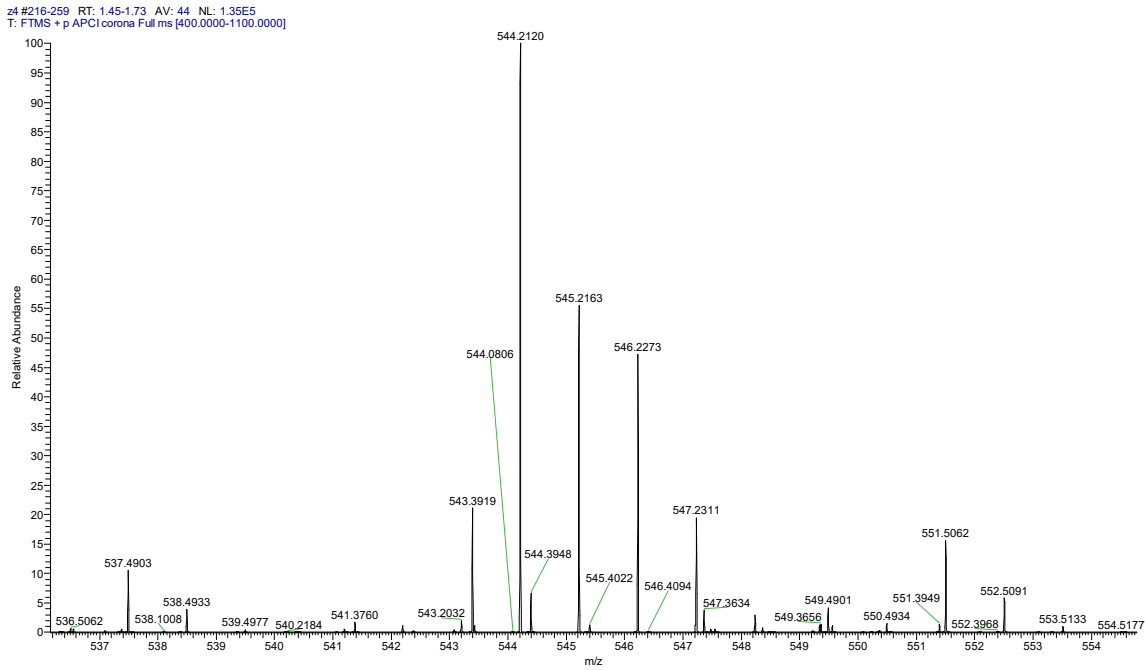
HRMS of 4a



HRMS of 4b



HRMS of 4c



HRMS of 4d

11. Reference

- (1) Miertus̄, S.; Scrocco, E.; Tomasi, J. *Chem. Phys.* **1981**, *55*, 117.
- (2) Cammi, R.; Tomasi, J. J. *Comput. Chem.* **1995**, *16*, 1449.
- (3) Tomasi, J.; Persico, M. *Chem. Rev.* **1994**, *94*, 2027.
- (4) Cramer,C. J.; Truhlar, D. G. *Chem. Rev.* **1999**, *99*, 2161.
- (5) Frisch, M. J.; Trucks, G. W.; Schlegel, H. B. Gaussian09, Revision A.01, Gaussian, Wallingford, Con, USA, **2009**.

Author Contributions

Weidong Zhang conceived the idea for the study. Guoqiang Li prepared the samples and conducted characterizations. Guoqiang Li, Yan Wang, Zengheng Wen, and Zhuang Luo helped to prepare and characterize the samples. Weidong Zhang and Guoqiang Li wrote the manuscript and Guoqiang Li, Yan Wang, Yaohui Li, and Weijun Song revised and polished the manuscript.